Engineered Science
DOI: https://dx.doi.org/10.30919/es1294

Simulation of Hot Casting Shrinkage of Thermoplastic Beryllium Oxide Slurries with Ultrasonic Activation

Uzak Zhapbasbayev,[1] Zamira Sattinova[2,*] and Gaukhar Ramazanova[1,*]

Abstract

The article proposes a method for calculating the shrinkage of hot casting of thermoplastic beryllium oxide slurries. The thermoplastic slurry (hereinafter referred to as slurry) is a composition system with a dispersed phase (binder) having a low thermal conductivity compared to the dispersed phase (beryllium oxide). Ultrasonic treatment reduces the viscosity of the slurry and improves its casting properties. The hot casting of beryllium oxide slurry is carried out without breaking the continuity of the system and depends on speed and temperature factors. Cooling-solidification of the slurry in the casting unit takes place in stages in a liquid state, a crystallization state with a phase transition, and a plastic state of the casting. The cooling rate of the casting at all stages depends on the design of the cavity, the rheological properties of the slurry, and the casting speed. The novelty of the work is the determination of shrinkage by the distribution of the concentration of the kinetically free binder. The slurry near the cooled wall is in a state of crystallization and plasticity, and the other part may still be in the liquid phase. Along the cavity cross-section, there is the inhomogeneous distribution of temperature, density, and concentration of kinetically free binder. This leads to compensation of shrinkage by the inflow of slurry from the liquid into the crystallization zones and the plasticity of the casting.

Keywords: Hot casting; Thermoplastic slurry moulding; Shrinkage; Beryllium oxide; Ultrasonic activation.
Received: 23 June 2024; Revised: 08 October 2024; Accepted: 29 October 2024.
Article type: Research article.

1. Introduction

Beryllium oxide (BeO) ceramics are used in various devices as 1) refractory material of crucibles; 2) insulators-heat sinks, substrates of transistors and microcircuits; 3) windows and insulators for microwave technology; 4) dielectric discharge tubes, resonators and hollow dielectric waveguides; 5) heat pipes of cryogenic technology; 6) material of a fuel matrix element in nuclear reactors; 7) neutron reflector as part of neutron filters.[1-6]

Recently, beryllium oxide (BeO) has attracted much attention due to its outstanding properties, such as high hardness, high electrical resistivity, high thermal conductivity, high melting point, and excellent radiation resistance. Beryllium ceramics are widely used as structural ceramics (micro heat exchangers) for high-efficiency microwave devices, vacuum lamps, magnetrons, and gas lasers.[5] BeO also has a long history of use in the nuclear field for both fission energy production and fusion due to its excellent mechanical, thermal, and chemical properties. The excellent chemical compatibility of BeO and uranium dioxide (UO_2) allows the production of tolerant UO_2 and BeO fuels. UO_2 and BeO ceramics arranged in fuel rods have two main advantages: better thermal conductivity due to the existence of BeO and better ability to retain fission products.[7] When combined with BeO, the poor thermal conductivity of UO_2 could be effectively improved. In addition, BeO ceramics was one of the best candidates as neutron moderators, neutron reflectors, and nuclear fuel matrix materials in nuclear reactors.[7,8] Over the last few decades, the electronic, optical, and mechanical properties of BeO have been described in many experimental and theoretical works. Beryllium oxide is widely used in precision instruments, particularly in space guidance and control systems, where the material is required to be highly stable under high thermal stresses. In the refractory industry, beryllium oxide is considered one of the best refractory materials.[6]

The development of technology and equipment for casting

[1] *Scientific Laboratory "Energy Modeling", Satbayev University, str. Satbayev 22, Almaty 050013, Kazakhstan.*
[2] *Department of Power Engineering, Faculty of Transport and Energy, L.N. Gumilyov Eurasian National University, Astana 010008, Kazakhstan.*
**Email:* sattinova.kz@gmail.com (Z. Sattinova), gaukhar.ri@gmail.com (G. Ramazanova)

thermoplastic slurry is similar to technology and equipment for casting metals and plastics. The technologies of these processes have a long scientific history and great scientific achievements. However, the physical and chemical nature of plastics and metals is different from composite powder materials, including ceramics. In the case of highly thermally conductive materials, particularly beryllium oxide, information on the technology of ceramics production is insignificant and requires further improvement. Therefore, in the development of technology for molding ceramics by hot casting from the very beginning was put forward the task of theoretical and experimental study of processes, which in turn were created special equipment for casting ceramics in the plant "Ceramics".[6-9]

As the results of experimental studies show, the process of hot molding of thermoplastic slurry has very strict requirements on the properties of products. One of the factors of the technological process is the dependence of physical and chemical properties of the slurry on temperature, phase transformations of the liquid suspensions with the heat of crystallization, and changes in the temperature boundary conditions on the cooling circuits.[2,9-11]

During cooling-solidification, the volume of the slurry changes (shrinkage). Shrinkage occurs: 1) in the liquid state when cooling from the heating temperature to the crystallization temperature; 2) when changing the aggregate state of crystallization from liquid to plastic; 3) in the plastic state when cooling from the crystallization temperature to the solidification temperature.[12-15] All the above stages depend on a number of factors and are closely related. Shrinkage in the hot casting process is determined by the characteristics of the dispersion phase of the binder. Achieving shrinkage compensation is the main technological task.[12-15] The importance of this operation is due to the fact that in the absence or incomplete compensation of internal shrinkage, the latter is the cause of internal defects (shells, porosity) in castings and products.[14,15] Shrinkage compensation can be accomplished by the inflow of hot slurry into the liquid and crystallization zone of the slurry. In the plastic state, shrinkage compensation is created by a pressure gradient to squeeze the casting out of the moulding cavity.[14-16]

The article proposes a method of calculating the shrinkage of the slurry by developing a model of physical processes and computational experiments. As a result, it is possible to track in detail the changes in the temperature-phase fields of the process and clearly represent the shrinkage and solidification kinetics depending on casting modes and features of the casting configuration.

2. Experimental studies of the casting of beryllium oxide slurry

2.1 Pilot plant for slurry casting

A schematic description of the experimental installation is presented in Fig. 1.

The pilot plant includes a slurry tank 1, a die 2, a set of auxiliary equipment including a casting transportation unit 3, thermostats 4, and control devices.[6,9] The moulding cavity of the die has two zones through which the long product is continuously extruded: the pre-treatment zone, where the slurry is in a liquid state, the moulding zone, where the casting is formed by cooling the slurry. In the die zone, ultrasonic treatment of the slurry is carried out by magnetostrictive transducer 5 and ultrasonic generator 6. Pressure on the surface of the slurry in tank 1 is created by compressed gas (air, nitrogen) supplied through the gas distribution system. Ultrasonic generator USG-4 (power $P = 0.1 - 4$ kW, frequency $f = 18 - 22$ kHz, working voltage $U = 220 \pm 44$ V, magnetizing current $I = 18 \pm 3$A) is used as a power supply source for acoustic systems. The main parameters of the installation are given.[6] Resistance thermometers, thermoregulators, and potentiometers are used to control and regulate water temperature in heating and cooling circuits.

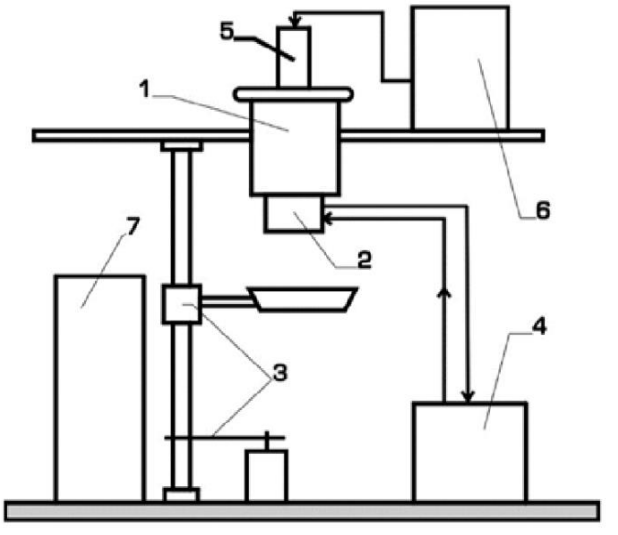

Fig. 1 Schematic diagram of a pilot plant for ultrasonic slurry casting: 1-slurry tank; 2-die; 3-casting transportation unit; 4-thermostat; 5-magnetostrictive transducer; 6-ultrasonic generators (USG-4); 7-control cabinet.

Experimental results show that the imposition of ultrasonic vibrations with an amplitude of 2 -6 μm, with a frequency of 50-100 Hz, reduces the viscosity of the wall layer of thixotropic slurry, respectively friction is reduced by 20-40 times.[6] For each slurry, there is an optimal vibration intensity, which can be realized by selecting the frequency and amplitude of vibration. Thus, at frequency $f = 50$ Hz and at vibration amplitude $A = 2 - 2.5$ mm, it is possible to obtain a viscosity reduction of 10 - 12 times. The possibilities of the experimental installation allow for the precise regulation of air pressure (1.0-100 MPa) and the conditions of heat exchange during the crystallization of the slurry (Q = 0.01-1.0 m^3/hour). The most significant impact of ultrasonic vibrations ($f = 16 - 18$ kHz) has on multi-component ligaments, and with an increase in the number of high-molecular compounds, this

effect is most pronounced in the first 5-10 min. treatment.[6] The thermoplastic slurry is a high-viscosity suspension consisting of organic binder and beryllium oxide powder (Table 1, specific surface area $1.72 \cdot 10^{-3}\ m^2/kg$). The organic binder consists of three components: paraffin, beeswax, and oleic acid in ratios (82, 15, and 3%).[6]

Table 1. Main characteristics of beryllium oxide powder.[6]

Bulk weight $\rho \cdot 10^3\ kg/m^3$		0.75
Specific surface, $S \cdot 10^{-3}\ m^2/kg$		1.72
	fraction in μm	%
	from 1.4	35.2
	1.4-4.2	52.7
Grain size distribution	4.2-7.0	9.6
	7.0-9.8	1.7
	9.3-12.6	0.4
	12.6-15.4	0.3
	15.4-18.2	0.1

Beryllium oxide powder has a particle size distribution by fractions (Table 1). The mass fraction of organic binder varies in the range $\omega = 0.100 - 0.117$. This composition of BeO powder shows satisfactory casting properties of the slurry at the change of mass fraction of binder from $\omega = 0.100$ to $\omega = 0.117$.

2.2 Experimental data on moulding of slurry

The moulding of the slurry was carried out in the experimental die (Fig. 2) by measuring the temperature using thermocouples along the height of the annular cavity.[9]

The experimental die is designed for casting a round tube with an outer diameter of $0.02\ m$ and an inner diameter of $0.012\ m$. The material of the mandrel and crystallizer is X18H10T steel, and the wall thickness of the crystallizer is $0.003\ m$. The total height of the cylindrical part of the annular cavity-$H = 0.028\ m$, the height of the hot zone of the annular cavity- $h_1 = 0.008\ m$, the height of the cold zone of the annular cavity-$h_2 = 0.020\ m$.[9] Water with temperature $t_1 = 80$ ºC. was supplied to the upper (hot) circuit of the crystallizer. In the lower (cold) circuit - water with temperature $t_2 = 20$ ºC. The maximum water throughput of the crystallizer circuits is $1500\ l/hour$.

The working tank connects the inlet conical part of the die of the casting unit, where the beryllium oxide (BeO) slurry is located. The slurry flows from the working tank into the inlet conical part of the annular cavity with the initial temperature $t_0 = 80$ ºC. As it moves due to heat exchange with the wall of the mandrel and the die, it changes its aggregate state and hardens. Table 2 shows the casting mode parameters. In the experiments, the casting speed varied from 0.020 to 0.100 m/min, and their effects on the thermal regime of the slurry formation were found. According to the experimental data, the boundaries of solidification of the slurry were obtained. Figure 3 shows the positions of the solidification zone: AB-isotherm of "fluid" (54 ℃), CD-isotherm of "solidus" (40 ℃), BS-bushing surface, MS-mandrel surface.

As can be seen from Fig. 3, the increase in casting speed leads to the expansion of the solidification zone and its displacement to the area of heat removal of the cold circuit. This is explained by the fact that with the increase in casting speed, the heat removal on the walls of the annular cavity does not have time to cool the slurry, and the solidification zone is stretched out and displaced downward in the direction of casting speed.

2.3 Rheological properties of beryllium oxide slurry

Exposure of oscillations on the slurry provides distribution of rheological properties of thermoplastic beryllium oxide slurry by changing the volume contents of solid and liquid phases. The composition and properties of the casting system are characterized by the concentration ratio of beryllium oxide powder - solid phase C_v and organic binder - liquid phase C_ω. Concentrations C_v and C_ω are determined by equations (1-2):

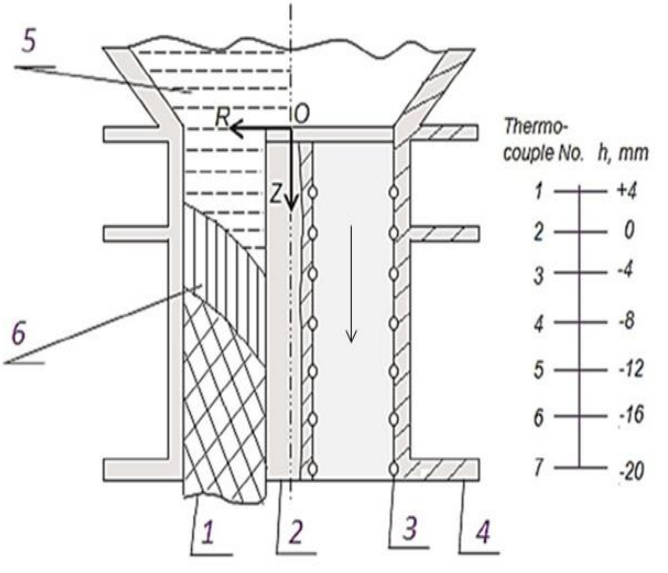

Fig. 2 Schematic diagram of a pilot die: 1-casting, 2-mandrel, 3-thermocouple, 4-crystallizer, 5-liquid slurry, 6-solidification zone.

Table 2. Experimental modes in the casting plant.[9]

Chart №1		1	2	3	4	5
Casting mode	Hot water flow, l/hour	500	500	500	500	500
	Cold water flow rate, l/hour	1500	1500	1500	1500	1500
	Casting speed, mm/min	20	40	60	80	100
	Hot water temperature (ºC)	80	80	80	80	80
	Cold water temperature (ºC)	20	20	20	20	20

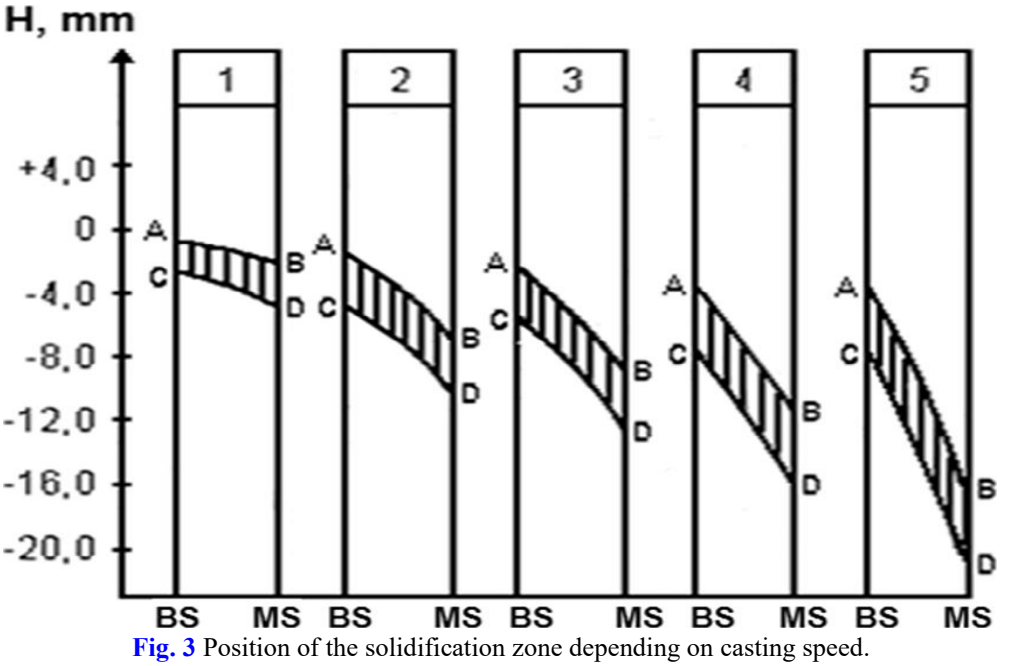

Fig. 3 Position of the solidification zone depending on casting speed.

$$C_v = \frac{V_{sl}-V_{bin}}{V_{sl}} = 1 - C_\omega \quad (1)$$

$$C_\omega = \frac{V_{sl}-V_{BeO}}{V_{sl}} \quad (2)$$

where V_{bin} and V_{BeO} are the volumes of binder and powder in slurry; V_{sl} is the slurry volume found from the expression:

$$V_{sl} = \frac{m_{sl}}{\rho_{sl}} = \frac{m_{BeO}}{m_{BeO}} + \frac{m_{bin}}{\rho_{bin}}, \qquad \omega = \frac{m_{bin}}{\rho_{bin}}$$

Substituting V_{sl} to formula (2), you can define C_v relative to the density of the solid phase and binder as equation (3):

$$C_v = 1 - \frac{\omega\rho_{BeO}}{(1-\omega)\rho_{sl}+\omega\rho_{BeO}} \quad (3)$$

where ω - relative mass content of binder, fractions of units.

According to the results of the experiments, the volume content % of the solid phase was calculated by formula (3) in the range of varying values of binder content (9.5 - 11.7% wt.) and temperature $(20 - 75\ ℃)$ (Table 3). The volume content of the solid phase at the initial temperature of 75 ℃ and the composition of the binder varies in the liquid slurry from 65.7 to 70.7 % (Table 3). The critical concentration of solid phase in the slurry C_v^s is the limiting concentration of beryllium oxide powders. The value C_v^s is equal to the relative density of the solid phase in the precipitate obtained by centrifugation of the slurry at a temperature of 90 ℃.[6]

Concentration of the liquid slurry C_ω is given by equation (4):

$$C_\omega = C_\omega^k + C_\omega^W \quad (4)$$

The kinetically bound part of the binder C_ω^w is solvated by beryllium oxide powder particles. Therefore, it goes through the whole moulding stage in the solid phase and hardens in the casting of the slurry. After the firing stage, it defines beryllium oxide ceramics.[6,12] The kinetic free part of the binder C_ω^k expresses the flowability of the slurry during the moulding process. The value C_ω^k changes during cooling and solidification of the slurry along the length of the cavity. Therefore, the temperature shrinkage of the slurry can be determined from the concentration distribution of the kinetically free binder C_ω^k .[6, 12] The volume fraction of kinetically free binder in the slurry is smaller the closer the volume fraction of the solid phase of the suspension is to the critical one and is determined by equation (5):[12]

$$C_\omega^k = 1 - n_v \quad (5)$$

where $n_v = \frac{C_v}{C_v^s}$ - relative fraction of solid phase concentration is in the slurry. Table 4 shows the experimental data of the parameters of the slurry composition depending on the content of the solid phase at a temperature of 75 ℃.

Table 3. Volumetric content of solid phase % slurries of different compositions depends on temperature.

Temperature, ℃	Binder density, g/cm^3	Content of binder, % by weight				
		9.5	10.0	10.3	10.7	11.7
20	0.924	74.3	73.2	72.5	71.7	69.6
40	0.900	73.8	72.6	72.0	71.1	69.0
55	0.788	71.1	69.9	69.2	68.3	66.1
60	0.783	71.0	69.8	69.1	68.2	66.0
63	0.780	70.9	69.7	69.0	68.1	65.9
66	0.777	70.8	69.6	68.9	68.0	65.7
75	0.773	70.7	69.5	68.8	67.9	65.7

The density of the binder components changes during the transition from liquid to plastic state. Fig. 4 shows a graph of the change in the density of binders and their components from temperature, obtained experimentally. The curve of the binder density dependence on temperature is described by spline functions as equation (6):

$$\rho_{bin} = 1.1987 - 0.0075\,t\ (20℃ \le t < 55℃)$$
$$\rho_{bin} = 1.0122t^{-0.063}(55℃ \le t < 76℃) \quad (6)$$

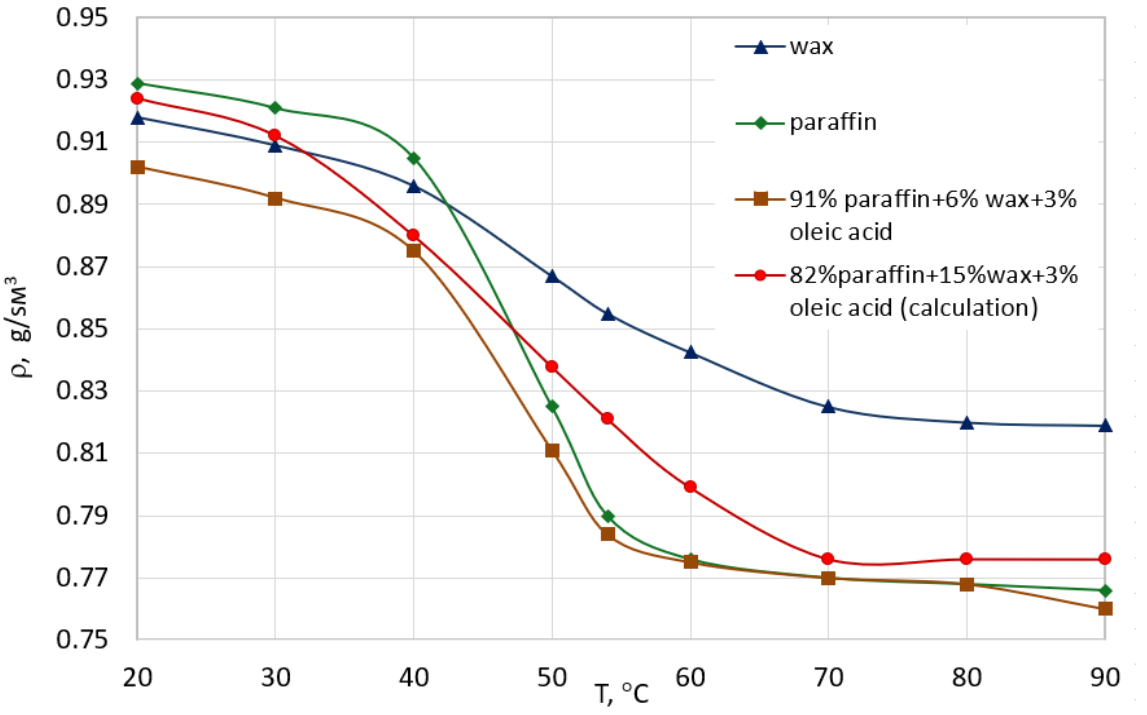

Fig. 4 Experimental data on the density of binders and their components as a function of temperature.

Table 4. Parameters of the slurry depend on the content of solid phase ($T = 75$ ℃).

ω, % binder mass fraction	C_v	C_v^s	$n_v = \frac{C_v}{C_v^s}$	C_ω^k	C_ω^W
1	2	3	4	5	6
11.7	0.657	0.723	0.908	0.092	0.251
10.7	0.679	0.728	0.932	0.068	0.253
10.0	0.695	0.734	0.946	0.054	0.251

In the process of cooling the binder from 75 to 20 ºC, the binder density increment is 1.20 (Table 4). Including cooling up to 55 ºC is 1.03, from 55 to 40 ºC-1.14, and from 40 to 20 ºC-1.03. The binder density increment at crystallization and plastic state of the slurry has a value of 1.17. Thus, according to experimental data, the interval below 55 ºC (crystallization zone and plastic state) accounts for up to 97.5% of the temperature shrinkage value. The density of the solid phase (BeO powder) is 3020 kg/m^3. The change in the density of the slurry depending on the temperature is determined by equation (7)

$$\rho_{sl} = \frac{\rho_{tv}\rho_{bin}}{(1-\omega)\rho_{bin}+\omega\rho_{BeO}} \quad (7)$$

Exposure of disperse systems to ultrasonic vibrations at a frequency of 18-22 kHz and power of 0.1-1.6 kW is accompanied by changes in their structure.[6,9,17] Experimental study of viscosity changes in time showed that the decrease in viscosity of the slurry is clearly manifested in the first 5-15 min of ultrasonic treatment (Fig. 5). Decrease in viscosity of the slurry (time of ultrasonic treatment 5-15 min.) is associated with intensive mass exchange processes at the interface of phases with different characteristics (solid dispersed phase and dispersion medium). The viscosity will decrease during movement until the structure is completely destroyed. However, the viscosity will gradually increase. At laminar flow in the temperature range $59-75$ ºC and at constant pressure, the viscosity of the slurry mass depends significantly on the US exposure time and shear rate. The graphs of experimental data show that there is a non-monotonic change in viscosity depending on the duration of US exposure (Fig. 5).[17]

Rheological parameters of the slurry $\mu_p(Pa\cdot s)$, $\tau_0(Pa)$ at mass fraction of binder $\omega = 0.100, \omega = 0.117$ and duration of 15 minutes of ultrasonic treatment, taken on viscometers, were approximated by empirical formulas.

Dependences of plastic viscosity $\mu_p\,(Pa\cdot s)$, yield strength $\tau_0\,(Pa)$, heat capacity $c_p\,(J/kg\cdot$℃) and thermal conductivity $\lambda(W/m\cdot$℃) on temperature for binder $\omega = 0.100$ are described by equations (8):

$$\mu_p(t) = 4440.958\cdot\exp(-0.09068\cdot t)$$
$$\tau_0(t) = 762.1393\cdot\exp(-0.04968\cdot t)$$
$$c_p(t) = 1000\cdot\exp(0.0034\cdot t) \quad (8)$$
$$\lambda(t) = 7.1exp(-0.01\cdot t)$$

and for binder $\omega = 0.117$ are described by equations (9):

$$\mu_p(t) = 625.044\cdot exp(-0.0708\cdot t)$$

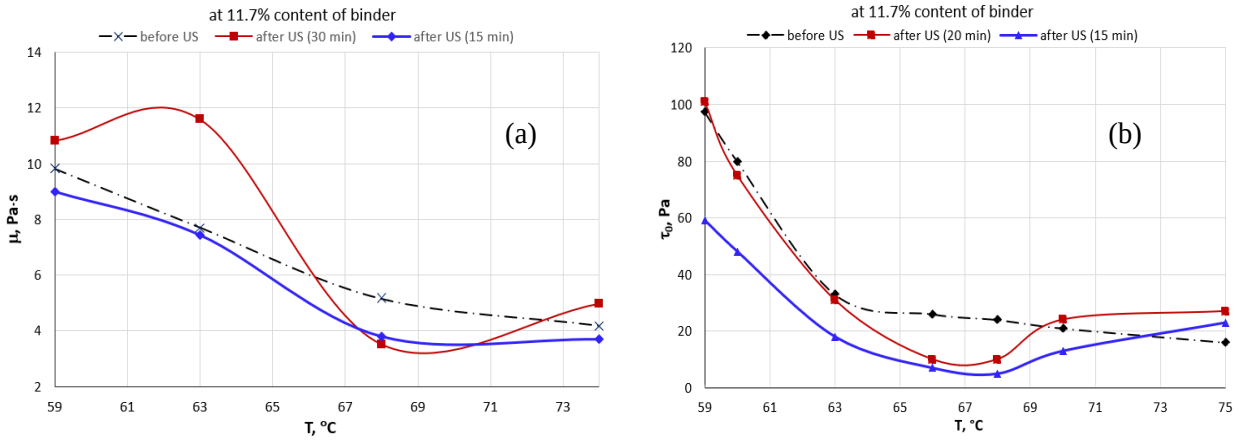

Fig. 5 Changes of viscosity (a) and yield strength, (b) depending on temperature and duration of US processing.

$$\tau_0(t) = 18.1 + 8.3 \cdot exp[-(t-69)/4.8]$$
$$c_p(t) = 70 + 1070 \cdot exp(0.0027 \cdot t) \quad (9)$$
$$\lambda(t) = 1.6 + 4.8 \cdot exp(-0.017 \cdot t)$$

Empirical equations (8) and (9) obtained by generalizing experimental data are used to close the mathematical model.

3. Mass and heat transport model

3.1 Problem statement

Forming of thermoplastic beryllium oxide slurry takes place in the cooled cavity of the die of the plant (Fig. 6). The cavity has a circular (Fig. 6a) or annular shape (Fig. 6b). The cooling circuit consists of two parts of hot and cold water. The circular cavity has a radius $r_1 = 0.006\,m$, length $L = 0.050\,m$ for a binder with mass fraction $\omega = 0.100$ and length $L = 0.089\,m$ for a binder with mass fraction $\omega = 0.117$, respectively. The annular cavity has radii $r_1 = 0.015\,m$, $r_2 = 0.018\,m$, length $L = 0.050\,m$ for binder with mass fraction $\omega = 0.100$ and length $L = 0.089\,m$ for binder with mass fraction $\omega = 0.117$, respectively.

The liquid slurry flows into the die cavity with an initial temperature t_0. As it moves, the slurry mass cools and solidifies.

The slurry takes a structural shape at the outlet of the circular cavity in the form of a rod (Fig. 6a) and in the form of a tube at the outlet of the annular cavity (Fig. 6b).

3.2 Rheological model of beryllium oxide slurry

In experiments,[6,9] beryllium oxide slurry has the property of a viscoplastic liquid. Therefore, the effective molecular viscosity of the slurry can be written as equation (10):[17-20]

$$\mu_{eff} = \begin{cases} \mu_p + \tau_0 |\dot{\gamma}|^{-1}, & if\ |\tau| > \tau_0, \\ \infty, & if\ |\tau| \le \tau_0 \end{cases} \quad (10)$$

For a Newtonian fluid, the yield strength $\tau_0 = 0$ and the effective viscosity are constant and equal to the molecular viscosity of the corresponding fluid. The Schwedoff-Bingham model is a simple viscoplastic fluid model that linearly relates the yield shear stress to the viscosity.[17-20] Expression (10) at $\tau \le \tau_0$ tends to infinity. Therefore, in accordance with the approach,[21] we present it in the form:

$$\mu_{eff} = \mu_p + \tau_0 \frac{1 - exp(-10^3 |S|)}{|S|} \quad (11)$$

This effective viscosity equation (11) makes it possible to carry out calculations for Schwedoff-Bingham liquids.

3.3 Basic equations

The equation of motion (13) can be written in the narrow channel approximation,[9,22] taking into account the expression of the effective viscosity (10).

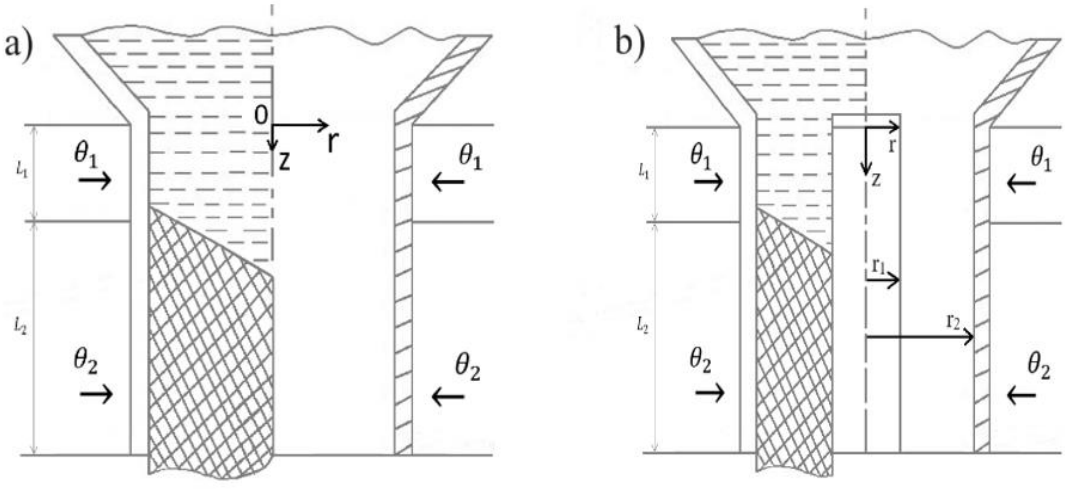

Fig. 6 Diagram of the die (a) circular cavity, (b) annular cavity.

$$\frac{\partial \rho u}{\partial z} + \frac{1}{r}\frac{\partial r \rho v}{\partial r} = 0 \quad (12)$$

$$\rho u \frac{\partial u}{\partial z} + \rho v \frac{\partial u}{\partial r} = -\frac{dp}{dz} + \frac{1}{r}\frac{\partial}{\partial r}\left(r \mu_{eff} \frac{\partial u}{\partial r}\right) + \rho g \quad (13)$$

As experiments show, the aggregate state of the slurry ranges in the temperature from 59 to 54 ºC.[6,11] In this case, the heat of phase transition can be accounted for by the model of apparent heat capacity.[23-26] Heat transfer occurs along the radius and length of the cavity due to the cooling of the cavity. The heat transfer equation (14), taking into account the assumptions made, can be written in the cylindrical coordinate system:[26]

$$\rho u c_p \frac{\partial t}{\partial z} + \rho v c_p \frac{\partial t}{\partial r} = \frac{\partial}{\partial z}\left(\lambda \frac{\partial t}{\partial z}\right) + \frac{1}{r}\frac{\partial}{\partial r}\left(r \lambda \frac{\partial t}{\partial r}\right) + \mu_p \left(\frac{\partial u}{\partial r}\right)^2 \quad (14)$$

where z, r -axial and radial coordinates; u, v - velocity components; $p, \rho, t, c_p, \mu_{eff}, \mu_p, \lambda$ - slurry parameters.[14] The pressure gradient (15) is found from equation (12) of the mass flow rate conservation condition:[26]

$$\int_S \rho u dS = \rho_0 u_0 S \quad (15)$$

where S - is the cross-sectional area of the cavity.

Thus, the system of equations (5)-(15) constitutes a mathematical model of the process of hot casting of thermoplastic beryllium oxide slurry.

3.4 Boundary conditions

Boundary conditions of the problem are standard. At the cavity inlet, the axial velocity component is equal to the casting velocity, and the radial component is zero. The temperature of the slurry is equal to $t_0 = 75$ ºC. On the walls of the cavity for the velocity of the slurry in the liquid state are put the conditions of adhesion, and in the zones of crystallization and solidification - the conditions of sliding.

In the zone of hot contour on the outer wall of circular and annular cavity for temperature Neumann's condition is put. In the zone of the cold contour of the cavity on the outer wall, the heat transfer conditions are set for the temperature as equation (16):

$$-\lambda \frac{\partial t}{\partial r} = k(t - \theta_2) \quad (16)$$

where k - transfer coefficient, θ_2 - cold water temperature.

A Neumann condition is placed on the axis of the circular cavity and on the inner wall of the annular cavity. At the outlet of the circular and annular cavity, soft conditions are set. The heat of phase transition during slurry crystallization is considered by the apparent heat capacity method, and the calculated results are given.[9]

3.5 Numerical method of solution

The system of equations of continuity (12), motion (13), and heat transfer (14) is solved by numerical method. The region under consideration is divided into unit cells with sides Δzi and Δrj. The Crank-Nicolson method is used to obtain the finite-difference equation of motion (13).[26] The difference analog of equation (12) is obtained by a two-layer scheme of the second order of accuracy.[26] The splitting method is used to calculate the pressure gradient from the condition of conservation of mass flow (15).[20,26] The finite-difference analog of the heat transfer equation (14) is obtained by the control volume method. The convective terms of the heat transfer equation (14) are approximated by a counter-flow scheme of the second kind, and the conductive terms by a scheme of the second order of accuracy.[26] The difference analogs of the equation of motion (13), continuity (12), and heat transfer equation (14) are considered together since the density $\rho(t)$, plastic viscosity $\mu_p(t)$, yield strength $\tau_0(t)$, heat capacity $c_p(t)$, heat conductivity $\lambda(t)$ depends on the temperature of the slurry. The iterative process is constructed as follows:

1) Solving the heat transfer equation (14) to determine the value of t_{ij}^n, the lower index i, j is the specific grid cell, and the upper index n is the iteration level;

2) Using the found temperature value, the values of density $\rho(t_{ij}^n)$, plastic viscosity $\mu_p(t_{ij}^n)$, yield strength $\tau_0(t_{ij}^n)$, heat capacity $c_p(t_{ij}^n)$, thermal conductivity $\lambda(t_{ij}^n)$ are found;

3) Solving the equation of motion (13) and conservation of mass (15) to determine the value of u_{ij}^n, pressure gradient $\left(\frac{dp}{dx}\right)_i^n$;

4) Solving the continuity equation (12) to determine the value of v_{ij}^n;

5) From the found values of u_{ij}^n, v_{ij}^n plastic viscosity $\mu_p(t_{ij}^n)$, yield strength $\tau_0(t_{ij}^n)$, effective viscosity can be determined $\mu_{eff}(t_{ij}^n)$.

The iterative process continues until the maximum error in determining t_{ij}^n, u_{ij}^n, v_{ij}^n does not satisfy the convergence condition $\varepsilon < 10^{-6}$. A non-uniform mesh (in both axial and radial directions) was used, and mesh refinement was applied in the inlet and near-wall regions. For all numerical investigations performed in this study, a base mesh with 1000×80 along the axial and radial directions was used. The convergence of the mesh was tested for three mesh sizes: coarse 750×50 and fine 1500×120. Numerical calculations were performed using the "in-house" code.

4. Discussion of the calculated data

4.1 Calculation data in a circular cavity

Figures 7 and 8 show the calculated data in the circular cavity with the cavity radius $r_1 = 0.006\ m$, length $L = 0.050\ m$ for link with mass fraction $\omega = 0.100$. The casting velocities were $u = 0.120\ m/min$ (Fig. 7) and $u = 0.160\ m/min$ (Fig. 8). The temperature of the slurry at the inlet to the circular cavity is constant along the section and is equal to $t_0 = 75$ ºC. In the first cooling circuit, the wall temperature is equal to $\theta_1 = 75$ ºC (Fig. 7a). In the second cooling circuit, the water temperature is $\theta_2 = 34$ ºC. Heat exchange occurs between cold and warm environments.[26] This can cause the temperature in the hot zone to drop from 75 to 72 ºC. In the cold zone, dynamic viscosity $\mu_p(t)$, density $\rho(t)$, and ultimate yield strength $\tau_0(t)$ increase with decreasing temperature. The slurry slides along the cavity walls along the length of the second circuit. This causes the profile of the

longitudinal velocity component downstream to become constant across the cavity cross-section.

The growth of wall heat removal in the second cooling circuit leads to a decrease in the temperature field (Fig. 7a). In this area, the temperature decreases from 72 to 34 ºC, and there is a change in the aggregate state of the slurry.[6,9] Cooling of the slurry leads to a decrease in temperature at the outer wall, while in the rest of the cavity, the temperature of the slurry will be higher (Fig. 7a). Therefore, the temperature field along the cavity cross-section will be inhomogeneous. While near the outer wall the slurry will crystallize and solidify, in the rest of the cavity the slurry may still be in a liquid state (Fig. 7a). Such temperature distribution of the slurry is in qualitative agreement with the calculated data.[26] The temperature field determines the inhomogeneous distribution of the slurry density along the cavity cross-section (Fig. 7b). The density of the slurry increases along the length of the circular cavity during the transition from liquid to crystallization zone and plastic state (Fig. 7b).

The sliding of the slurry on the wall ensures the continuity of the medium and provides the structural shape of the casting without warping. The density increment is 1.055 and corresponds to the experimental data for the mass fraction of binder $\omega = 0.100$.[6]

The concentration distribution of the kinetically free binder C_{ω}^{k} is shown in Fig. 7c. It can be seen that the concentration C_{ω}^{k} decreases along the length of the circular cavity from $0.054\ to\ 0.0$. As an interpretation of the experimental data on shrinkage compensation depending on the composition of the slurry, the data of castings with higher density achieved due to deformed compaction of the slurry during structure formation are given. Increasing the density of the casting under conditions of homogeneous cooling due to changes in the volume-phase structure under the influence of ultrasound is a more effective compensation for shrinkage during solidification. Compensation for shrinkage during casting with ultrasound is achieved by feeding the casting with liquid slurry, as well as by deformed compaction of the slurry during structure formation of the casting.

To test the mechanism of deformation compensation of shrinkage, the samples cast without ultrasound were placed in a special mold and subjected to hydrostatic compression on the unit at a pressure of 5 MPa and a temperature of 40 ºC. The increase in the density of the casting under hydrostatic compression (Table 5), taking into account the rheological characteristics of the slurry in the temperature of the casting structure formation, we can consider that the deformation mechanism of the slurry compaction is one of the main one in shrinkage compensation. The given experimental dependences[6] and the data in Table 5 indicate a better compensation of shrinkage in 1.5-2 times for the samples formed from the slurry with a high 11.2% binder content, which is due to the optimal combination of the used modes of ultrasonic treatment and the composition of the slurry.

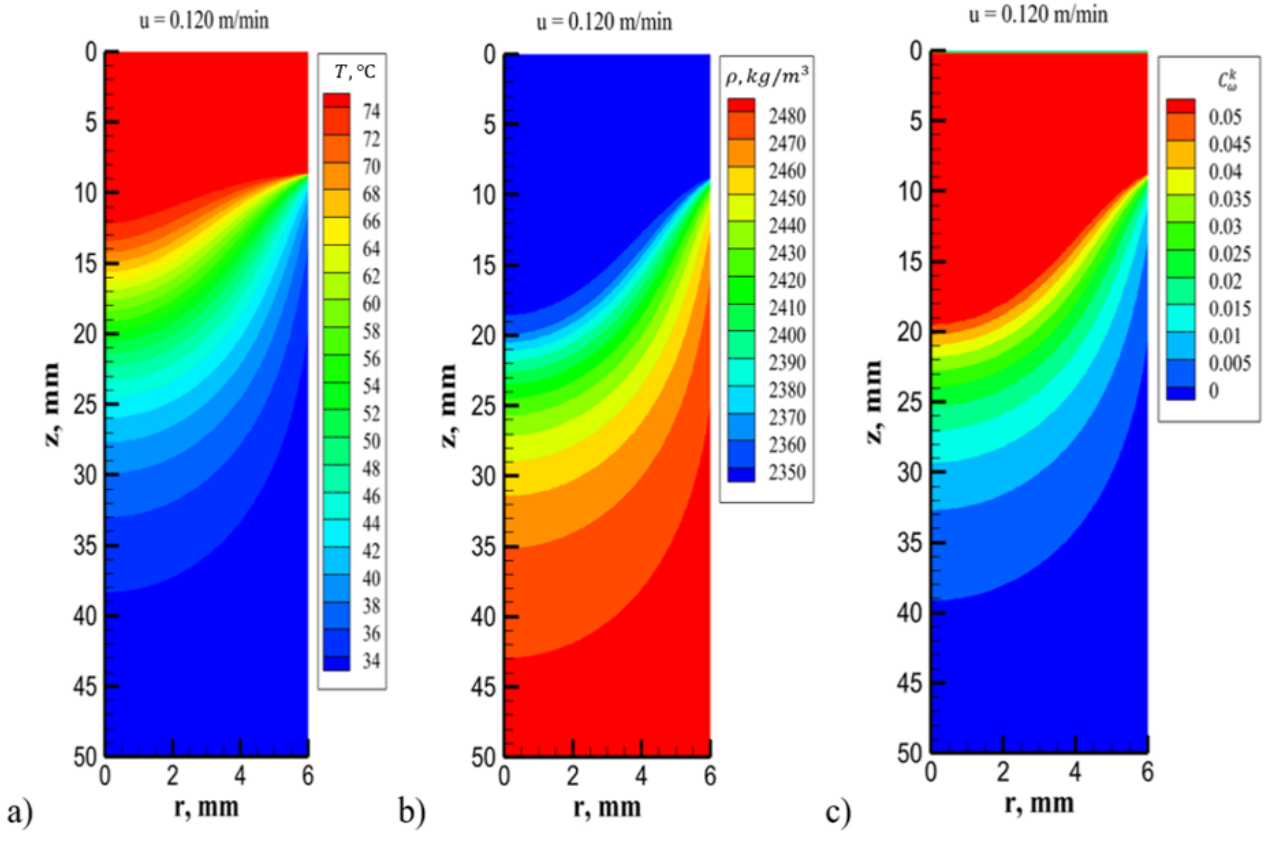

Fig. 7 The field of temperature, density, and kinetically free concentration of slurry in the circular cavity with the mass fraction of the binder $\omega = 0.100$.

Table 5. The apparent density of castings and semi-finished products after pre-firing.

Acoustic-technological scheme	ω, % weight fraction of binder	apparent density of the slurry in a liquid state		apparent density				relative density of castings	
				during US processing		with hydrostatic additional pressing			
		calc	fact	castings	semi-finished product	castings	semi-finished product	at US	at hydros compres
	9.5	2.36	2.36	2.37	2.30	2.42	2.31	95.6	97.6
	11.2	2.28	2.28	2.39	2.31	2.40	2.30	98.0	98.4

The above fact allows us to recommend for die casting of castings from thermoplastic BeO-based slurry, when using ultrasonic treatment, the use of a slurry with a high binder content of 11.2-11.7%.

The distribution C_ω^k shows the change of shrinkage along the length of the circular cavity. Near the outer wall, the shrinkage decreases rapidly to a limiting value ($C_\omega^k = 0$), while the inhomogeneous distribution of shrinkage occurs in the rest of the circular cavity (Fig. 7c), which explains the distribution of the slurry temperature (Fig. 7a). It should be noted that along the length of the circular cavity, the shrinkage decreases to the limit value.

An increase in the casting rate (u=0.160 m/min) leads to an increase in the region of variation of temperature (Fig. 8a), density (Fig. 8b), and kinetically free binder concentration C_ω^k (Fig. 8c). These figures show the transition of the liquid slurry into crystallization and plasticity states. Along the length of the cavity, the density of the slurry increases from 2350 to 2480 kg/m^3, and the density increment is 1.055. The concentration of kinetically free binder C_ω^k (Fig. 8c) decreases from 0.054 to 0.0. The concentration distribution C_ω^k determines the shrinkage in the liquid zone, crystallization state, and plasticity of the slurry.

Figures 9 and 10 show the calculated data in a circular cavity for a binder with mass fraction $\omega = 0.117$. In the second cooling circuit the water temperature is $\theta_2 = 20$ ºC. The radius and lengths of the cavity are $r_1 = 0.006m$, $L = 0.089m$.

Casting rates and temperatures in the hot cooling circuit are the same as in the case of $\omega = 0.100$. Increasing the mass fraction of $\omega = 0.117$ binder of the slurry contributes to the cooling-curing rate. This can be seen from the temperature distribution for both casting rates. A inhomogeneous temperature field can also be seen here (Fig. 9a, Fig. 10a).

The density of the slurry increases from 2260 to 2480 kg/m^3, *i.e.*, the density increment is 1.097 for both casting rates (Fig. 9b, Fig. 10b). The concentration of kinetically free binder c_ω^k decreases from 0.092 to 0.0. Within the moulding

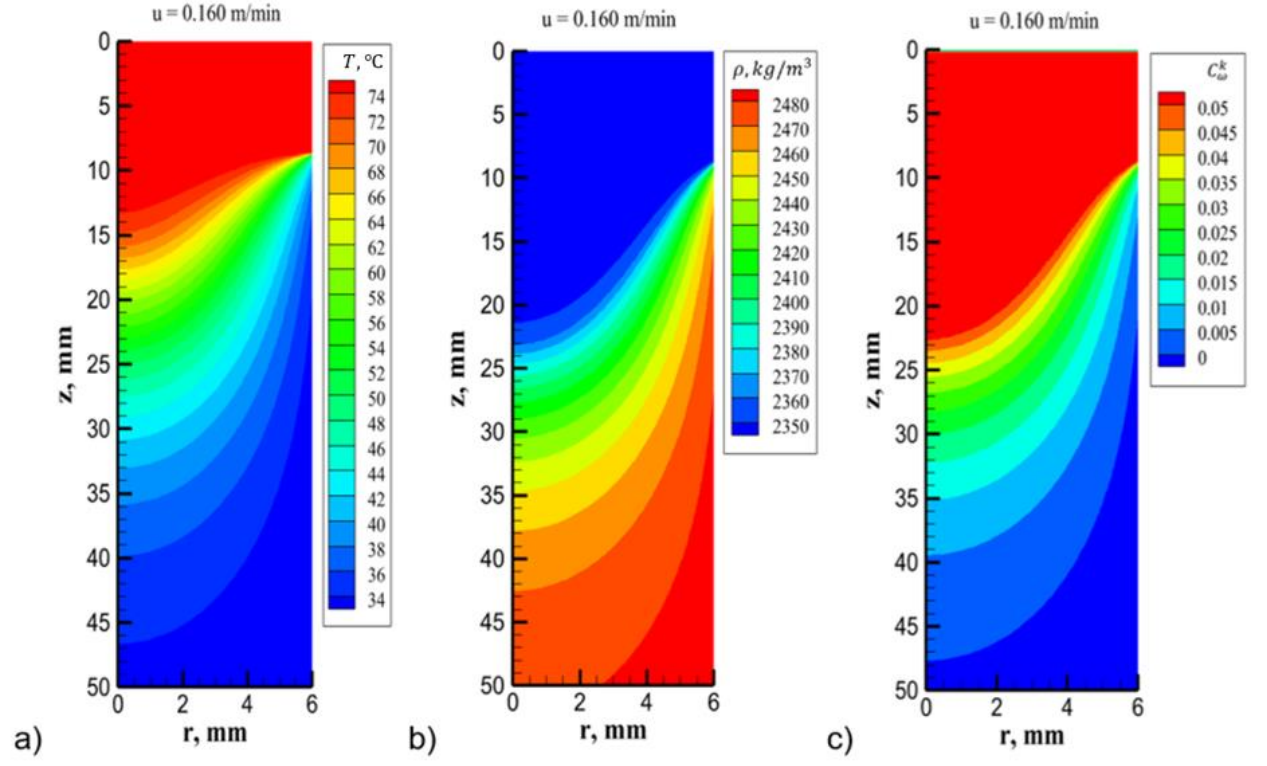

Fig. 8 The field of temperature, density and kinetically free concentration of slurry in the circular cavity at the mass fraction of the binder $\omega = 0.100$.

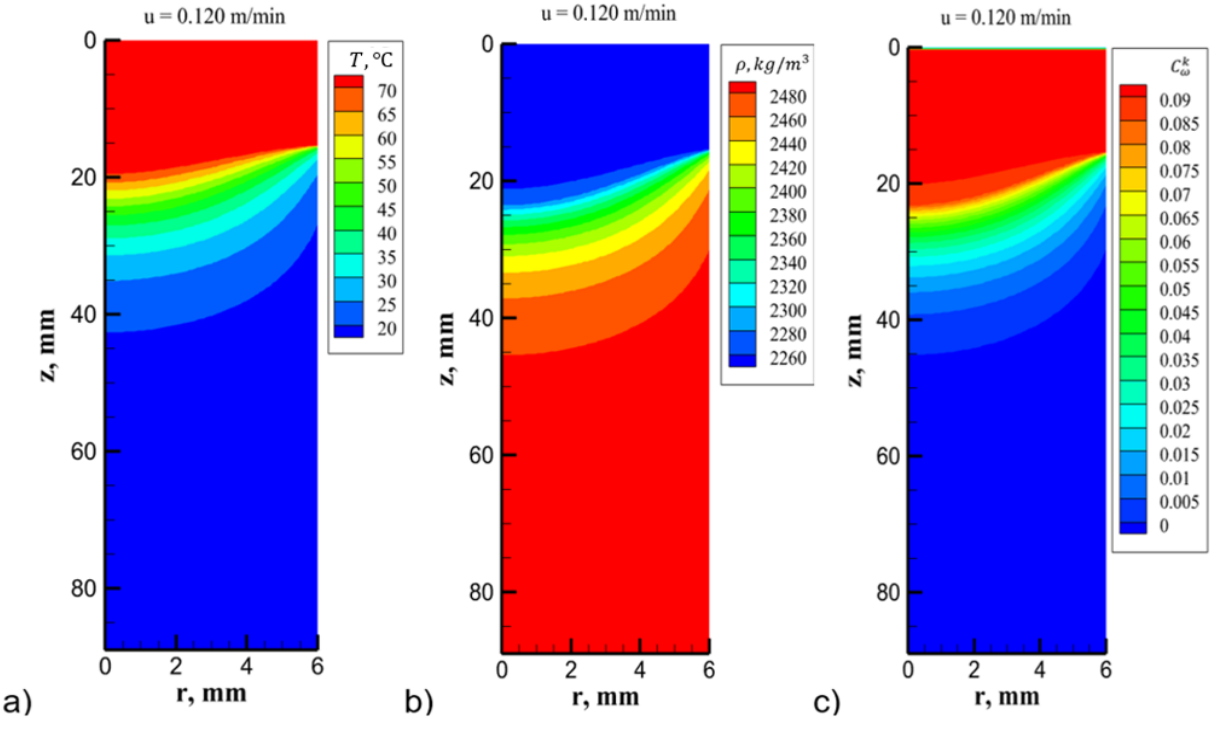

Fig. 9 The field of temperature, density and kinetically free concentration of the slurry in the circular cavity at the mass fraction of the binder $\omega = 0.117$.

cavity, the change c_ω^k determines the shrinkage in the liquid zone, crystallization state and plasticity of the slurry (Fig. 9c, Fig. 10c). The density increment is 1.097 and corresponds to the experimental data for the mass fraction of binder $\omega = 0.117$.[6]

4.2 Calculation data in the annular cavity

Figures 11 and 12 show the calculated data in the annular cavity for the binder with mass fraction $\omega = 0.100$ and $\omega = 0.117$, respectively. The casting speed was equal to $u = 0.245\ m/min$. The water temperatures in the cooling circuits were $\theta_1 = 75$ ℃,

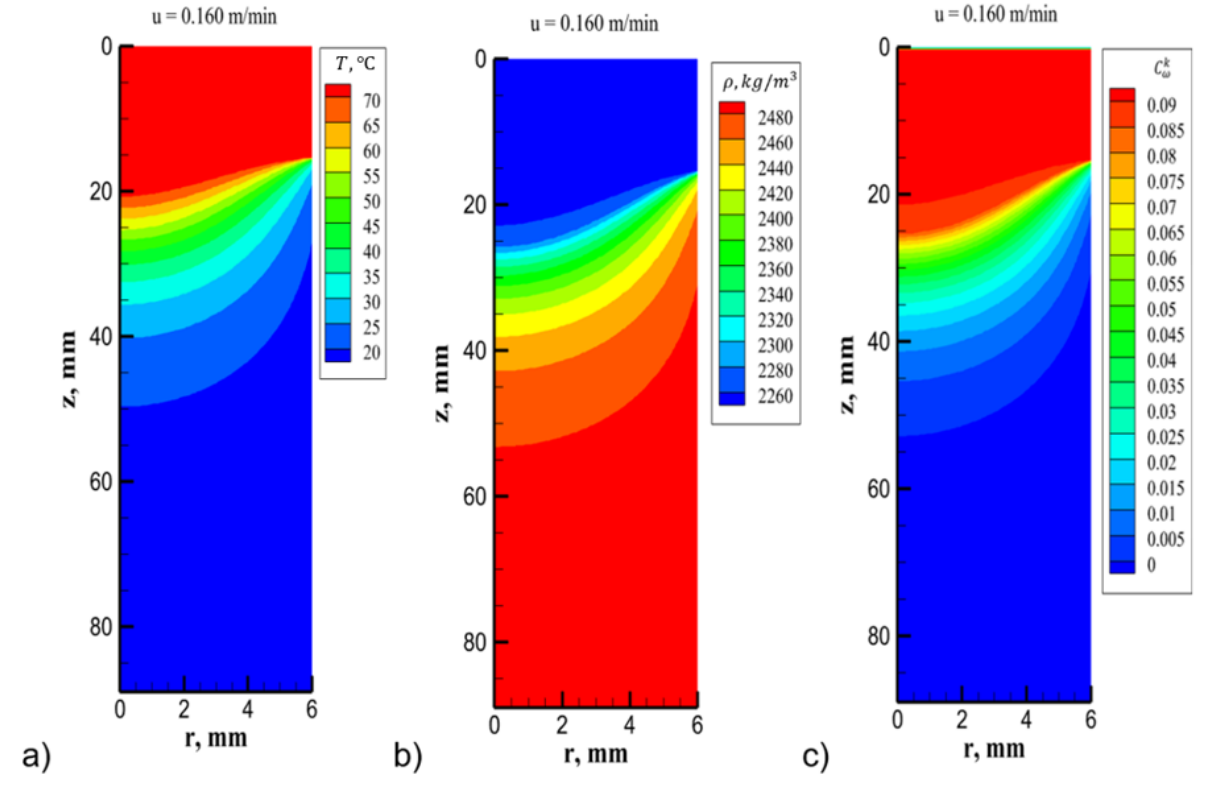

Fig. 10 The field of temperature, density and kinetically free concentration of the slurry in the circular cavity at the mass fraction of the binder $\omega = 0.117$.

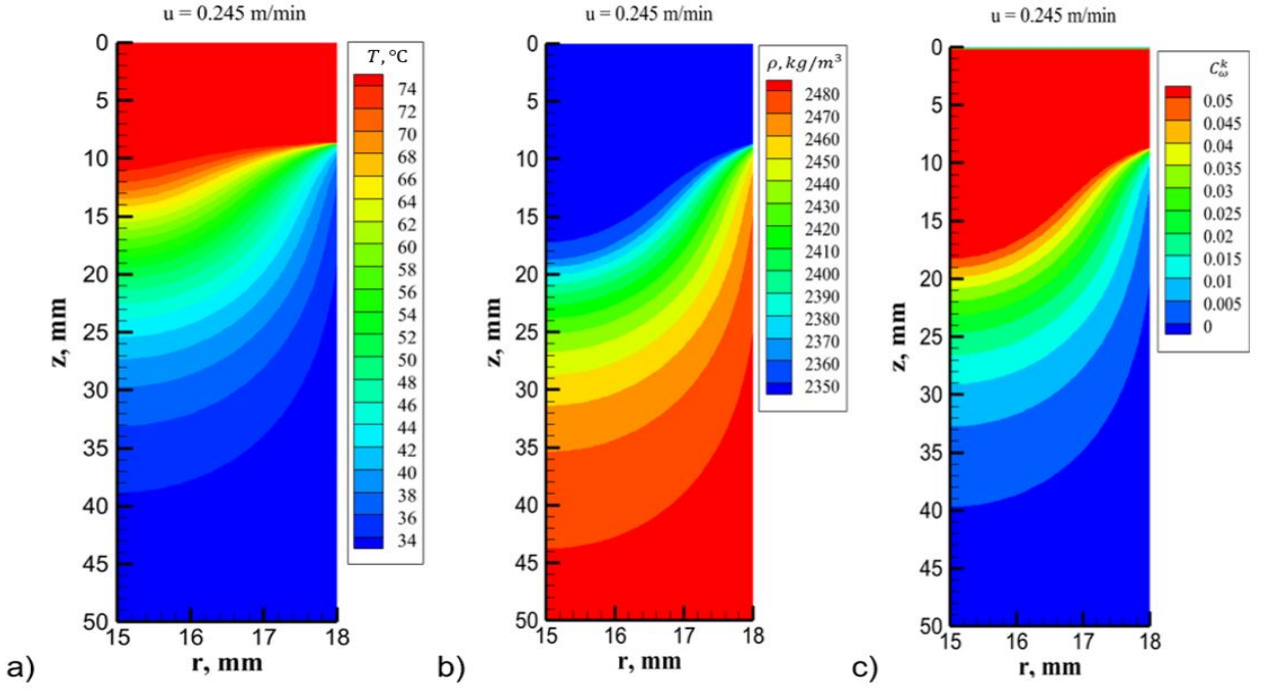

Fig. 11 The field of temperature, density and kinetically free concentration of the slurry in the annular cavity at the mass fraction of the binder $\omega = 0.100$.

$\theta_2 = 34\,℃$ for $\omega = 0.100$ and $\theta_1 = 75\,℃$, $\theta_2 = 20\,℃$ for $\omega = 0.117$.

As can be seen from Figs. 11 and 12, the temperature, density and kinetic free binder concentration fields describe the moulding process within the length of the annular cavity. Heat exchange along the outer contour of the annular cavity enhances the cooling-solidification of the slurry and leads to inhomogeneous temperature distribution in the annular cavity (Fig. 11a, Fig. 12a). The temperature field of the slurry determines inhomogeneous distributions of density and concentration of kinetically free binder c_ω^k along the length of the annular cavity. For the mass fraction of binder $\omega = 0.100$, the concentration of kinetically free binder C_ω^k varies from 0.054 to 0.0 and the density increment is 1.055.

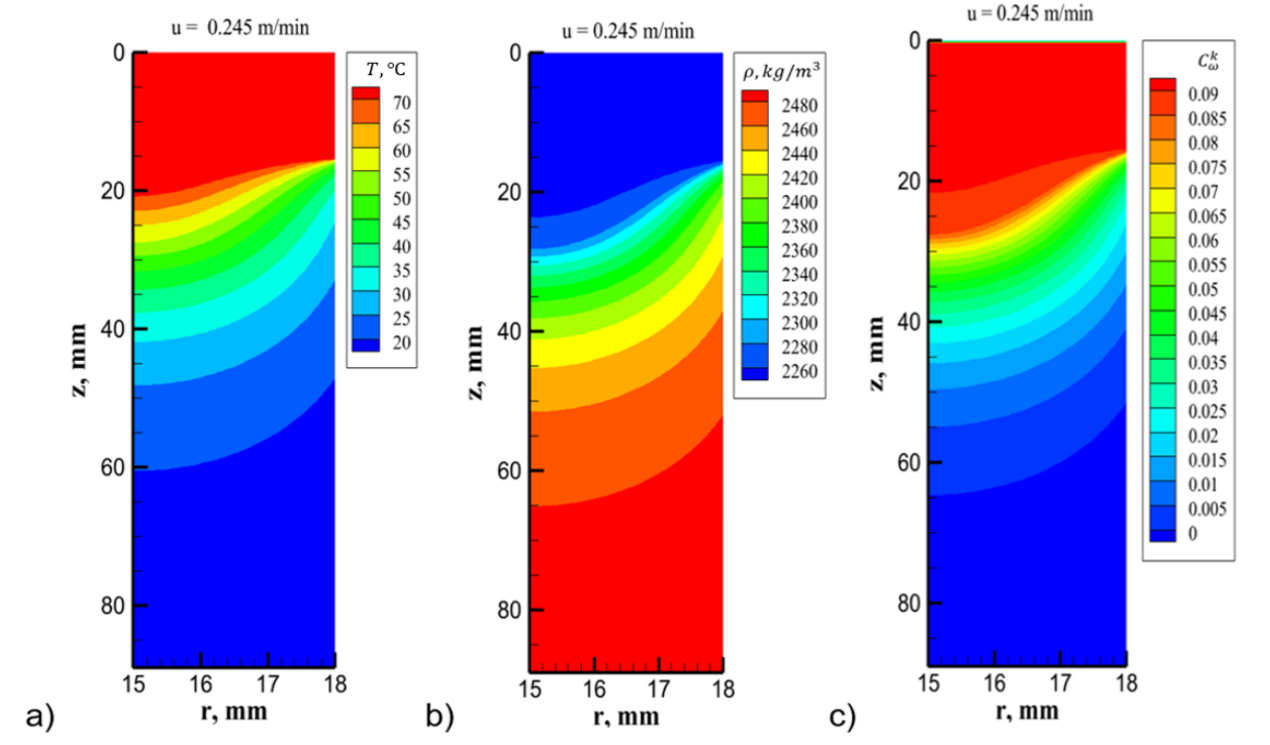

Fig. 12 The field of temperature, density, and kinetically free concentration of the slurry in the annular cavity with the mass fraction of the binder $\omega = 0.117$.

For the mass fraction of binder $\omega = 0.117$, the concentration of kinetically free binder changes from 0.092 to 0.0, and the density increment will be 1.097. Within the forming cavity, the change C_ω^k determines the shrinkage in the liquid zone, crystallization state, and plasticity of the slurry (Fig. 11c, Fig. 12c).

4.3 Comparison with production data

Comparison of calculations with production data was carried out in the annular cavity. Calculations were carried out at the mode parameters of production data (Table 6).

Figure 13 shows the results of calculations for mass fraction of binder $\omega = 0.100$ In the first cooling circuit, the wall temperature is $\theta_1 = 75$ ºC. The temperature field t shows a decrease from 75 to 72 ℃ (Fig. 13a), and the density field $\rho(t)$ uncreases from 2350 to 2360 kg/m^3(Fig. 13b). The concentration of kinetically free binder C_ω^k decreases from 0.054 to 0.050 (Fig. 13c). The shrinkage can be determined from the change in the concentration of the kinetically free binder C_ω^k. In the liquid zone, the shrinkage is 0.050 and can be compensated by the inflow of liquid slurry. In the second cooling circuit the wall temperature is $\theta_2 = 34$ ºC. The temperature of the slurry t decreases from 72 to 34 ℃ (Fig. 13a), and density $\rho(t)$) increases from 2360 to 2480 kg/m^3 (Fig. 13b).

The concentration of kinetically free binder C_ω^k decreases from 0.050 to 0.0 and determines the shrinkage in the crystallization zone and plastic state of the slurry. The calculated data for the mass fraction of the binder $\omega = 0.117$ are given in Fig. 14. Decreasing the temperature t of the slurry in the annular cavity from 75 to 20 ℃ leads to an increase in the density of the slurry $\rho(t)$ from 2260 to 2480 kg/m^3. The concentration of kinetically free binder C_ω^k decreases from 0.092 to 0.0 and expresses temperature shrinkage.

In the calculations, the density increment for the mass fraction of binder $\omega = 0.100$ is 1.055, and for the mass fraction of binder $\omega = 0.117$ is 1.097.

Table 6. Parameters of the slurry according to the production data.[6]

№	Content of binder in slurry, mass fraction	Slurry viscosity at $T_0 = 75$℃, Pa · s	Casting capacity slurry, mm	Casting speed, mm/min	Mechanical bending strength of casting, MPa
1	0.100	6.78	50	185	9.33
2	0.117	2.80	89	165	8.17

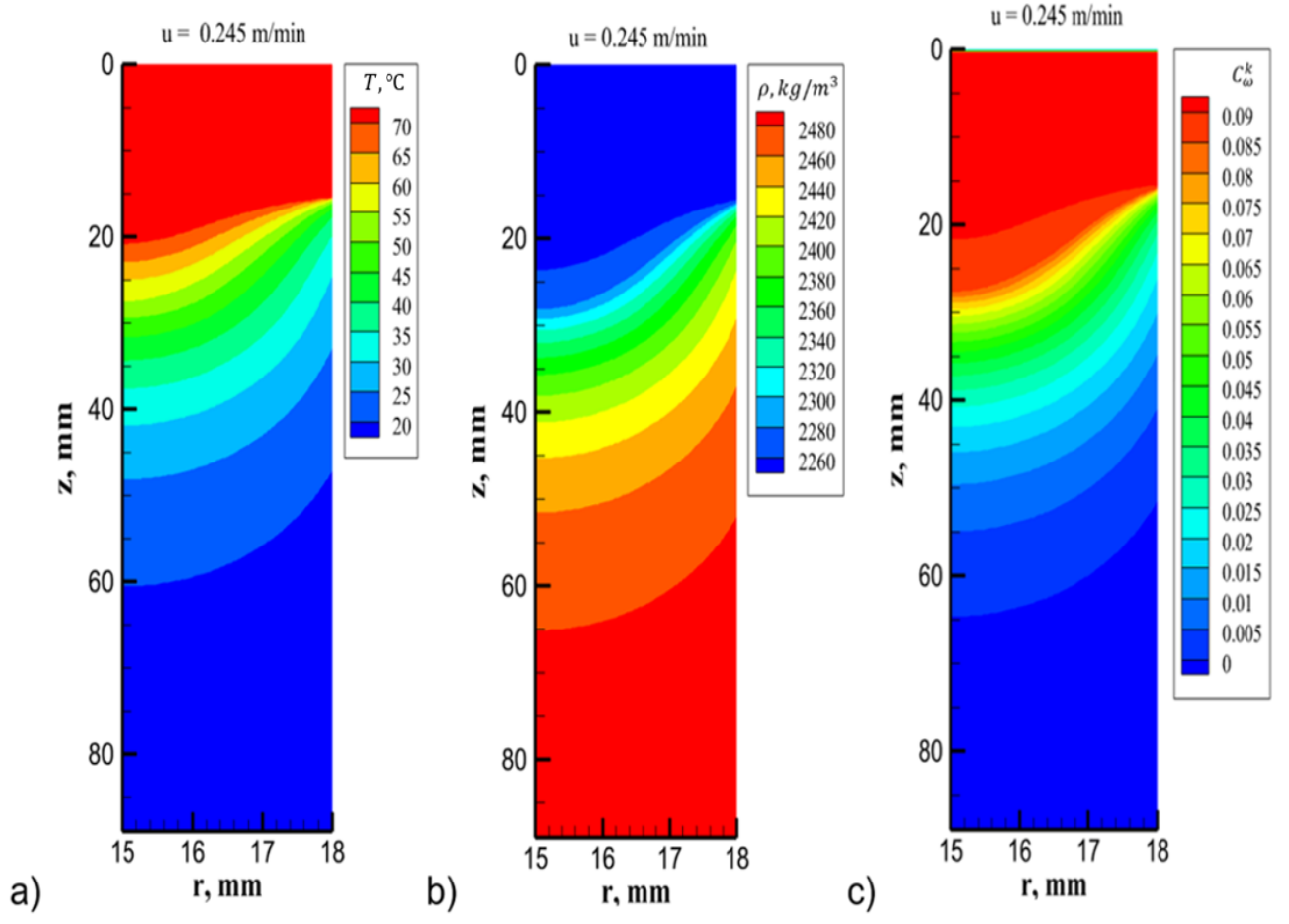

Fig. 13 Calculated data of temperature, density, and kinetically free concentration of slurry in the annular cavity at a mass fraction of binder $\omega = 0.100$.

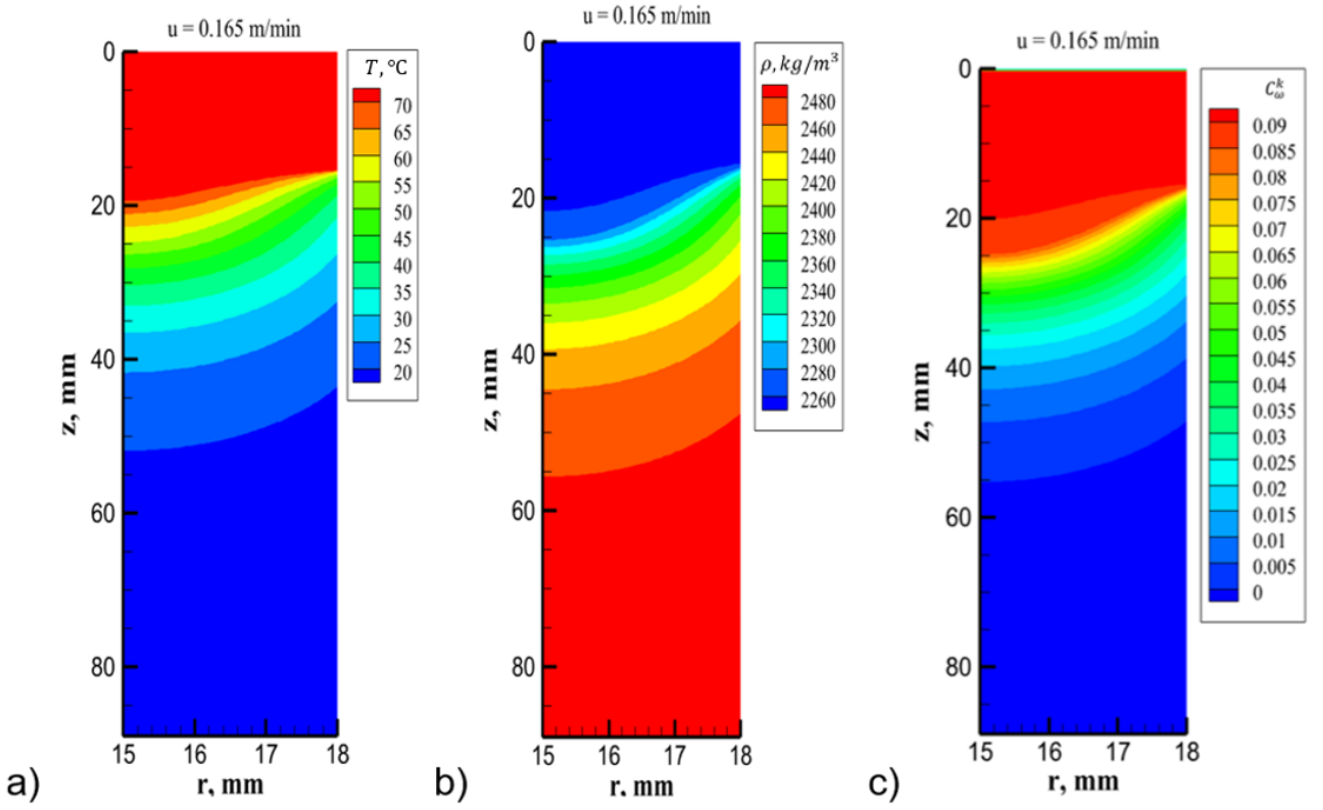

Fig. 14 Calculated data on temperature, density, and kinetically free concentration of slurry in the annular cavity at the mass fraction of the binder $\omega = 0.117$.

5. Conclusions

In this study, shrinkage calculations based on the distribution of the concentration of kinetically free binder were performed to mold a homogeneous structure of beryllium ceramics and to predict the occurrence of inhomogeneity and shrinkage shells that develop into finished products during solidification. Solidification of a casting does not occur immediately over its entire cross-section. It begins in the surface layer, then passes to the deep layers, and ends in the areas that are the thermal centers of the casting.

In the case of thermoplastic beryllium oxide resin casting, shrinkage compensation by the "make-up" method is the most common practice. However, for a number of products (*e.g.*, core, a ball), it is technically difficult to organize the required cooling for the casting. The scheme of shrinkage compensation by means of "under-pressing" provides for cutting off the sprue from the molding cavity after completion of filling and holding under pressure to reduce the volume of the casting during shrinkage of the slurry. The advantages of this shrinkage compensation mechanism include the independence of shrinkage compensation efficiency from the product shape. However, there is little information on the practical use of technical solutions for the realization of this shrinkage compensation mechanism. The correct selection of casting parameters plays an important role in optimal process flow and obtaining high-quality casting.

A considerable amount of work is devoted to the experimental study of the influence of the main casting: pressure and temperature conditions on the casting process and properties of castings. In practice, a wide range of temperatures (60-90 ºC) and pressures (1-100 atm.) recommended for the casting process has been established. However, despite the variation in the parameters, most researchers are generally the same in their assessment of the nature of the influence of temperature regimes and casting pressure on the casting process and the properties of castings. Thus, in particular, increasing the temperature of the slurry leads to some increase in the density of the semi-finished product. However, at the same time, the probability of internal sinks and friability increases sharply due to increased shrinkage of the slurry during cooling. The temperature field of cooling and solidifying slurry mass depends on the totality of thermophysical, geometric, and physicochemical factors of the foundry system, so it occupies a central place in all theoretical and experimental studies of the solidification process. In practice, up to 80% of volumetric changes associated primarily with the thermophysical properties of beryllium oxide occur in the temperature range 59-40 ºC. The above assumption is confirmed by the fact that the values of internal shrinkage vary significantly depending on the degree of compensation of volumetric changes occurring at the 1st and 2nd stages: volume reduction during cooling from the initial temperature $t = 75$ ºC to the temperature of the beginning of the change of the aggregate state $t = 59$ ºC, during the change of the aggregate state in the temperature range $t = 59 - 45$ ºC; in the solid (viscoplastic) state during

cooling to the final temperature $t = 20$ ºC in the molding cavity. In the next steps, binder removal, bound thermal process, and sintering by appropriate heating take place. Finally, this paper concludes with the shrinkage calculations of hot casting of thermoplastic beryllium oxide slurries in two molding cavities of the casting unit.

The results of calculations show the whole stage of hot casting moulding of beryllium oxide slurry taking into account the change of its aggregate state. Ultrasonic treatment improves the rheological properties and increases the flowability of the slurry in the moulding cavity.

Calculations show the influence of velocity, temperature factors and design data of the cavity on the cooling-solidification process of the casting. In a circular cavity at casting speeds $u = 0.120\, m/min,\ 0.160\, m/min$ and the mass fraction of binder $\omega = 0.100,\ \omega = 0.117$ inhomogeneous distributions of temperature, density and concentration of kinetically free binder C_ω^k are obtained. The temperature shrinkage of the slurry was found from the concentration distribution of kinetically free binder C_ω^k. In the annular cavity at casting speed, $u = 0.245\, m/min$ and the mass fraction of binder $\omega = 0.100$ and $\omega = 0.117$ inhomogeneous distributions of temperature, density and concentration of kinetically free binder C_ω^k are obtained. According to the change in the concentration of kinetic free binder C_ω^k, the shrinkages in the zones of liquid phase, crystallization, and plastic state of the slurry were determined. In calculations the conditions of moulding with shrinkage of slurry by hot casting method were found, which allow to obtain at the cavity outlet a solidified product with a homogeneous structure of beryllium oxide.

Acknowledgements

The numerical results of this research were funded by the Committee of Science of the Ministry of Science and Higher Education of the Republic of Kazakhstan, grant number AP19680086 for 2023-2025.

Conflict of Interest

There is no conflict of interest.

Supporting Information

Not applicable.

References

[1] R. G. Larson, Y. Wei, A review of thixotropy and its rheological modeling, *Journal of Rheology*, 2019, **63**, 477-501, doi: 10.1122/1.5055031.

[2] U. K. Zhapbasbaev, G. I. Ramazanova, Z. K. Sattinova, Mathematical model of hot-cast molding of ceramic, *Glass and Ceramics*, 2011, **68**, 216-220, doi: 10.1007/s10717-011-9356-2.

[3] V. S. Kiiko, V. Y. Vaispapir, Thermal conductivity and prospects for application of BeO ceramic in electronics, *Glass and Ceramics*, 2015, **71**, 387-391, doi: 10.1007/s10717-015-9694-6.

[4] G. P. Akishin, S. K. Turnaev, V. Y. Vaispapir, M. A. Gorbunova, Y. N. Makurin, V. S. Kiiko, A. L. Ivanovskii, Thermal conductivity of beryllium oxide ceramic, *Refractories and Industrial Ceramics*, 2009, **50**, 465-468, doi: 10.1007/s11148-010-9239-z.

[5] M. Vajdi, M. Shahedi Asl, S. Nekahi, F. Sadegh Moghanlou, S. Jafargholinejad, M. Mohammadi, Numerical assessment of beryllium oxide as an alternative material for micro heat exchangers, *Ceramics International*, 2020, **46**, 19248-19255, doi: 10.1016/j.ceramint.2020.04.263.

[6] S. A. Shakhov, A. E. Gagarin, Rheological characteristics of thermoplastic disperse systems treated with ultrasound, *Glass and Ceramics*, 2008, **65**, 122-124, doi: 10.1007/s10717-008-9030-5.

[7] M.-D. Hou, X.-W. Zhou, B. Liu, Beryllium oxide utilized in nuclear reactors: part I: Application history, thermal properties, mechanical properties, corrosion behavior and fabrication methods, *Nuclear Engineering and Technology*, 2022, **54**, 4393-4411, doi: 10.1016/j.net.2022.07.017.

[8] X.-W. Zhou, M.-D. Hou, R. Liu, B. Liu, Fabrication of beryllium oxide based fully ceramic microencapsulated nuclear fuels with dispersed TRISO particles by pressureless sintering method, *Journal of Nuclear Materials*, 2024, **588**, 154798, doi: 10.1016/j.jnucmat.2023.154798.

[9] U. Zhapbasbayev, G. Ramazanova, B. Kenzhaliev, Z. Sattinova, S. Shakhov, Experimental and calculated data of the beryllium oxide slurry solidification, *Applied Thermal Engineering*, 2016, **96**, 593-599, doi: 10.1016/j.applthermaleng.2015.11.114.

[10] G. P. Akishin, S. K. Turnaev, V. Y. Vaispapir, V. S. Kiiko, I. R. Shein, E. D. Pletneva, M. N. Timofeeva, A. L. Ivanovskii, Composition of beryllium oxide ceramics, *Refractories and Industrial Ceramics*, 2011, **51**, 377-381, doi: 10.1007/s11148-011-9329-6.

[11] U. K. Zhapbasbayev, A. Kaltayev, G. D. Bitsoev, S. K. Turnayev, Hydrodynamics of moulding of ceramic articles from beryllium oxide using ultrasonic activation, Proceedings of ASME 2005 International Mechanical Engineering Congress and Exposition, 2008.

[12] Y. E. Pivinskii, Volume phase characteristics and their effect on the properties of suspensions and ceramic casting systems, *Refractories*, 1982, **23**, 605-614, doi: 10.1007/BF01387481.

[13] Y. E. Pivinskii, E. M. Grishpun, A. M. Gorokhovskii, Engineering, manufacturing, and servicing of shaped and unshaped refractories based on highly concentrated ceramic binding suspensions, *Refractories and Industrial Ceramics*, 2015, **56**, 245-253, doi: 10.1007/s11148-015-9823-3.

[14] S. A. Shakhov, Controlling the deformation behavior of thermoplastic slips with ultrasound, *Glass and Ceramics*, 2007, **64**, 354-356, doi: 10.1007/s10717-007-0088-2.

[15] S. A. Shakhov, Use of ultrasound in order to intensify molding of high-temperature thermocouple sheaths, *Refractories and Industrial Ceramics*, 2008, **49**, 261-264, doi: 10.1007/s11148-008-9074-7.

[16] S. A. Shakhov, Mechanism for compensating slip volume

changes during hot casting of ceramic, *Glass and Ceramics*, 2007, **64**, 229-231, doi: 10.1007/s10717-007-0057-9.
[17] Z. K. Sattinova, T. N. Bekenov, B. K. Assilbekov, G. I. Ramazanova, U. K. Zhapbasbayev, Z. T. Nussupbek, Mathematical modeling of the rheological behavior of thermoplastic slurry in the molding process of beryllium ceramics, *Ceramics International*, 2022, **48**, 31102-31110, doi: 10.1016/j.ceramint.2022.07.178.
[18] E.C. Bingham, Fluidity and plasticity, McGraw-Hill, New York, 1922.
[19] A. Acrivos, Non-Newtonian fluids. Fluid mechanics, mixing and heat transfer, *International Journal of Heat and Mass Transfer*, 1962, **5**, 589, doi: 10.1016/0017-9310(62)90175-8.
[20] Z. K. Sattinova, T. N. Bekenov, B. K. Assilbekov, G. I. Ramazanova, K. M. Dyusenov, Development of the algorithm for calculating the optimal molding modes of the BeO slurry using various rheological models, *Bulletin of the Karaganda University Physics Series*, 2021, **104**, 85-93, doi: 10.31489/2021ph4/85-93.
[21] T. C. Papanastasiou, Flows of materials with yield, *Journal of Rheology*, 1987, **31**, 385-404, doi: 10.1122/1.549926.
[22] M. Jabbari, R. Bulatova, A. I. Y. Tok, C. R. H. Bahl, E. Mitsoulis, J. H. Hattel, Ceramic tape casting: a review of current methods and trends with emphasis on rheological behaviour and flow analysis, *Materials Science and Engineering: B*, 2016, **212**, 39-61, doi: 10.1016/j.mseb.2016.07.011.
[23] N. O. Moraga, R. A. Lemus-Mondaca, Numerical conjugate air mixed convection/non-Newtonian liquid solidification for various cavity configurations and rheological models, *International Journal of Heat and Mass Transfer*, 2011, **54**, 5116-5125, doi: 10.1016/j.ijheatmasstransfer.2011.07.032.
[24] T. Yamamoto, S. V. Komarov, Influence of ultrasound irradiation on transient solidification characteristics in DC casting process: numerical simulation and experimental verification, *Journal of Materials Processing Technology*, 2021, **294**, 117116, doi: 10.1016/j.jmatprotec.2021.117116.
[25] M. Carmona, C. Cortés, Numerical simulation of a secondary aluminum melting furnace heated by a plasma torch, *Journal of Materials Processing Technology*, 2014, **214**, 334-346, doi: 10.1016/j.jmatprotec.2013.09.024.
[26] T. Cebeci, P. Bradshaw, Physical and Computational Aspects of Convective Heat Transfer. New York, NY: Springer New York, 1988.